Applied Energy Symposium 2019: Low carbon cities and urban energy systems
October 16-18, 2019, Xiamen, China
Paper ID: 0207

MODELING STUDY OF LITHIUM-ION BATTERY BELOW ROOM TEMPERATURE

Bingxiang Sun[1,2], Zhenlin Zhu[1,2], Haijun Ruan[1,2],Tong Li[3], Xitian He[1,2], Xiaojia Su[1,2], Jian wu[1,2], Weige Zhang[1,2]

1 National Active Distribution Network Technology Research Center(NANTEC), Beijing Jiaotong University, Beijing, 100044, China
2 Collaborative Innovation Center of Electric Vehicles in Beijing, Beijing Jiaotong University, Beijing, 100044, China
3 Beijing Electric Vehicle Automobile Co., Ltd. Beijing, 102600, China

ABSTRACT

The battery model is the basis for battery state estimation, and its accuracy will directly affect the accuracy of the estimate. In the field of rail transit, combined with the actual operating conditions of the train to properly allocate the battery capacity, it is also necessary to establish an accurate battery model. At present, the commonly used battery model less considers the influence of temperature on the model parameters[1]. Because of the extreme low temperature conditions during the actual running of the train, this paper uses lithium iron phosphate battery as the research object, based on the second-order equivalent circuit model of the battery[2]. At the same time, considering the influence of low temperature on the available capacity of the battery[3], open circuit voltage, ohmic internal resistance and polarization parameters, a battery model suitable for room temperature below is proposed[4].

Keywords: LFP lithium-ion battery; Modeling below room temperature; Nernst equation; Arrhenius formula

1. SECOND-ORDER RC EQUIVALENT CIRCUIT MODEL

The Thevenin equivalent circuit model is the most common battery model in current battery modeling. However, it only uses a first-order RC loop to reflect the battery polarization process, and can not fully characterize the electrochemical polarization and concentration polarization behavior of lithium batteries[5]. In the actual chemical reaction process of lithium battery, the electrochemical polarization is determined by the activation energy of the electrochemical reaction of the electrode[6]. The electrochemical reaction rate of the positive and negative electrodes is less than the polarization caused by the electron motion rate, and the response time is short, which is reflected by the sudden change of the terminal voltage during the charging and discharging process[7]. Concentration polarization has a longer response time than electrochemical polarization, because the migration rate of lithium ions inside the electrode is much smaller than the electrochemical reaction rate occurring on the electrode surface, which is a slow and stable voltage process. The second-order RC model adds a first-order RC loop to the Thevenin model to describe the electrochemical polarization and concentration polarization processes[8]. Therefore, in order to more effectively describe the effects of different ambient temperatures on battery performance, this paper selects Based on the second-order RC model, a lithium iron phosphate battery model at low temperatures was established.

As shown in Figure 1, the second-order RC model

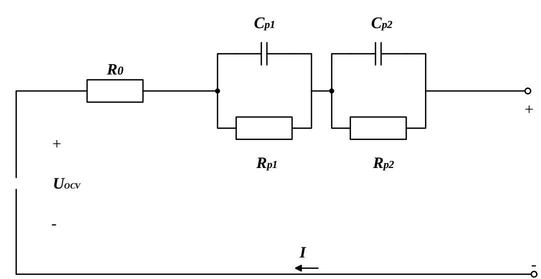

Fig 1 Second-order RC equivalent model.

consists of a controlled voltage source, an ohmic internal resistance, and two first-order RC networks. The controlled voltage source reflects the constraint relationship between the open circuit voltage and the SOC. Ohmic internal resistance consumes battery energy in the form of Joule heat during the chemical reaction. The second-order RC network reflects the overpotential caused by the electrochemical reaction imbalance inside the battery. The sum of the two partial overvoltages constitutes the polarization voltage.

Models can be described by these equations：

$$U = OCV - IR_0 - U_{P1}(t) - U_{P2}(t) \tag{1}$$

$$U_{P1}(t) = \begin{cases} R_{P1} * I(t) * (1 - e^{-(t-t_0)/\tau_1}) \\ U_{P1}(t_1) * e^{-(t-t_0)/\tau_1} \end{cases} \tag{2}$$

$$U_{P2}(t) = \begin{cases} R_{P2} * I(t) * (1 - e^{-(t-t_0)/\tau_2}) \\ U_{P2}(t_1) * e^{-(t-t_1)/\tau_2} \end{cases} \tag{3}$$

2. EXPERIMENTAL DESIGN

In this paper, ATL-78Ah lithium iron phosphate battery monomer was used as the experimental object. The battery experiment platform is built by using high and low temperature test box and ArbinBT-2000 charging and discharging test equipment.

The capacity calibration and parameter identification experiments were carried out on the battery at five characteristic temperature points of -20℃, -10℃, 0℃, 10℃ and 25℃ in the range of 25℃ to -20℃. In order to avoid the coupling effect of current rate and temperature on battery performance parameters, and consider the temperature rise caused by large-rate current discharge affects the accuracy of battery modeling, this paper uniformly uses 0.2C small rate current to discharge the battery, and lithium iron phosphate When the battery is less than zero, it is forbidden to charge at any rate. Therefore, this paper only considers the effect of temperature on the discharge performance of lithium iron phosphate. All charging experiments were carried out at 25℃ in a constant current-constant compression method with a standard charge rate of 0.2 given in the lithium iron phosphate manual[9].

First test the battery for low temperature capacity. The capacity of the battery at 10℃, 0℃, -10℃, -20℃ was measured by first charging at room temperature and

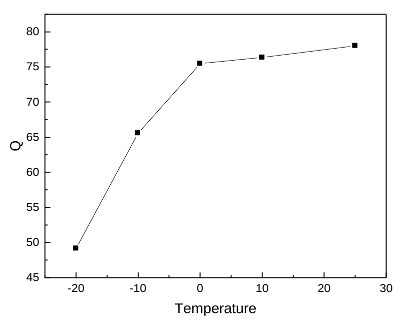

Fig 2 Line chart of battery capacity Q as a function of temperature.

then discharging below room temperature. The experimental results are shown in figure 2.

The second is the HPPC test. The battery is subjected to a discharge test at SOC=0, 0.1, 0.2, 0.3, 0.4, 0.5, 0.6, 0.7, 0.8, 0.9, and 11 points. The voltage and current of the battery are recorded and measured. The experiment is to prepare for the subsequent parameter identification. Through the data of the experiment, the parameters of the battery can be obtained through parameter identification.

3. PARAMETER IDENTIFICATION

In this paper, the open circuit voltage value after fully discharging after the battery is discharged is recorded as the OCV of the SOC characteristic point[10]. After sufficient standing, the voltage values on the polarization voltage and the ohmic internal resistance are both zero, and the voltage after standing is Zero, and the polarization process of the battery is completed, the external voltage measured at this time can be used as the OCV. The resulting OCV-SOC curve is shown

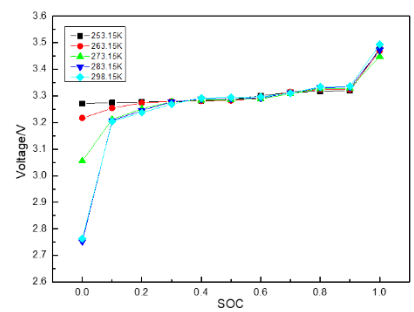

Fig 3 OCV-SOC graph

Moreover, the polarization internal resistance and polarization capacitance of each SOC feature point at different temperatures are obtained by least squares identification according to the polarization voltage expression. Then, the ohmic internal resistance is obtained by dividing the voltage jump within 1 s of the

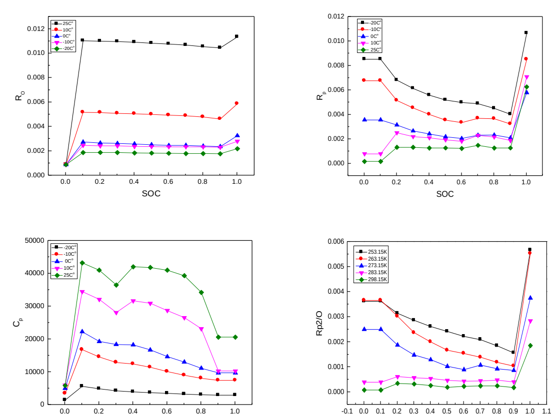

Fig 4 Ohmic internal resistance, polarization internal resistance, polarization capacitance-SOC curve

applied current and dividing the discharge current. The ohmic internal resistance, polarization internal resistance and polarization capacitance of the battery at different temperatures are identified as figure 4.

4. MODELING

4.1 Low-temperature battery usable capacity model

It can be seen from the experimental data that under the same conditions as the 25℃ experimental method, the amount of electricity discharged from the battery at a lower temperature is reduced, and the lower the temperature, the greater the volume reduction. Since the decrease of the available capacity of the battery at low temperature reflects the influence of temperature on the chemical reaction rate, this paper uses the empirical Arrhenius equation to curve the actual usable capacity of different temperature batteries[7].

$$Q_t / Q_0 = a * e^{-b/T} + c \tag{4}$$

This paper supplements the capacity test experiment with an ambient temperature of -5℃. The volume obtained by testing at four temperature points of -20℃, -10℃, -5℃, and 0℃ is fitted to a capacity curve below zero degrees Celsius. The volume obtained from the test at three temperature points of 0℃, 10℃ and 25℃ is fitted to a capacity curve above 0℃.

The fitting parameters are as follows:

Temperature	a	b	c
<0℃	-2.24119E-8	-4263.5428	86.00499
>0℃	187.35423	2403.8483	73.30047

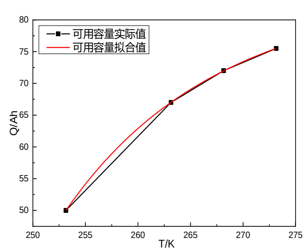

Fig 5 Subzero parameter

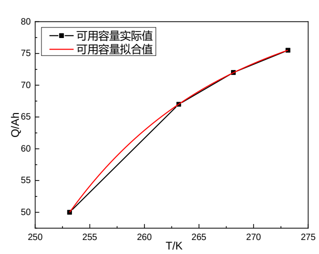

Fig 6 Parameters above zero zero

Figure 5 and Figure 6 show the capacity fit curves for the temperature range below zero and above zero:

The results show that the Arrhenius formula can be used to estimate the available capacity below room temperature to obtain more accurate results.

4.2 Low temperature battery OCV-SOC model

The Nernst equation indicates that in the reversible redox reaction of a lithium battery, there is a quantitative relationship between the cell electromotive force and the ions participating in the reaction:

$$OCV = OCV_0 - (RT_k / nF)\ln(\alpha_{fin} / \alpha_{fut}) \tag{5}$$

Among them, OCV represents the current battery open circuit voltage, OCV_0 represents the open circuit voltage when the battery is fully charged under the current temperature condition, T_k represents the current thermodynamic temperature, and R and F respectively represent the gas constant and the Faraday constant, which are constant values. α_{fin} and α_{fut} respectively indicate the lithium ion activity that has been reacted and has not yet participated in the reaction, and n indicates the number of electrons and electrons in the chemical reaction formula, which is involved in the reaction of lithium ions. The ratio of α_{fin} to α_{fut} can be expressed as the amount of electricity discharged by the battery and the remaining available capacity that can be released. Therefore, the formula can be converted into the relationship between the open circuit voltage and the SOC at a certain time of the lithium battery.

$$U_{oc}[SOC(t)]{=}a(T) + b(T) * \ln(SOC(t)) + c(T) * \ln(1 - SOC(t)) \tag{6}$$

a(T)、*b(T)* and *c(T)* represent the coefficients of the OCV-SOC equation at different temperatures. Based on the identification results of 11 SOC feature points OCV at five characteristic temperatures, the coefficients *a(T)*、*b(T)* and *c(T)* are obtained by least squares method. The parameters vary little between the two temperatures, so the parameters a, b, and c of the unknown temperature point in the model are obtained by piecewise linear

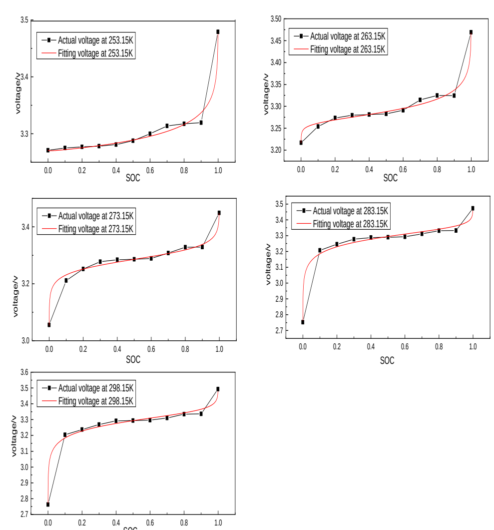

Fig 7 SOC-OCV fitting results at various characteristic temperatures

interpolation from *a*, *b*, and *c* obtained at the characteristic temperature point，The Nernst equation parameters are as follows：

Temperature/K	a	b	c
253.15	3.267880	-0.00044	-0.030036017
263.15	3.272568	0.006107	-0.028261767
273.15	3.287355	0.025453	-0.023286919
283.15	3.323194	0.060922	-0.019509659
298.15	3.318302	0.059417	-0.023362391

Figure 7 shows the results of SOC-OCV fitting at each characteristic temperature. According to the data analysis, the error of fitting the OCV of the Nernst equation is below 0.1%, which verifies the accuracy of the Nernst equation. Therefore, it is feasible to apply the Nernst equation and the model.

4.3 Battery low temperature internal resistance model

The ohmic internal resistance of eleven SOC feature points at five characteristic temperatures of -20℃, -10℃, 0℃, 10℃, and 25℃ can be obtained from the HPPC test. As shown in Figure 8.

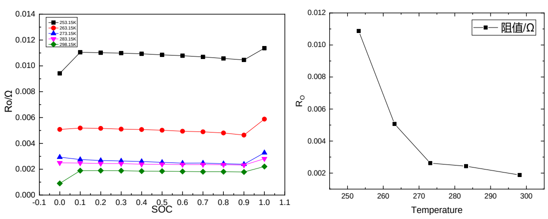

Fig 8 Internal resistance and Average internal resistance

It can be seen from the figure that although the internal resistance is affected by temperature, especially below zero degrees Celsius, for the same characteristic temperature point, the internal resistance changes little during the process of SOC decreasing from 0.9 to 0.1, taking SOC from 0.1 at each characteristic temperature. To the internal resistance value of the 0.9 interval, the average internal resistance value is obtained as shown in Fig. 8. In the model, the same internal resistance value can be used for different SOC points. For the relationship between the internal resistance and the temperature, the introduction of Arrhenius The Uz formula fits the curve:

$$R_T = Ae^{B/T} + C \tag{7}$$

Where R_T represents the ohmic internal resistance of the battery when the temperature is T, and A, B, and C are coefficients. In order to improve the accuracy, the parameters *A*, *B*, and *C* are identified based on the 11 SOC feature points during parameter identification. The results are as follows:

SOC	A	B	C
0	6.86E-09	3719.107891	0
0.1	6.86E-09	3719.107891	0
0.2	1.46E-07	2904.384152	0
0.3	1.70E-07	2849.800303	0
0.4	1.67E-07	2843.523281	0
0.5	1.71E-07	2826.687349	0
0.6	1.72E-07	2818.643713	0
0.7	2.86E-07	2691.623971	0
0.8	2.61E-07	2711.085558	0
0.9	2.60E-07	2697.267962	0
1	2.60E-07	2697.267962	0

The reason for obtaining the parameter list of this Arrhenius formula is that the internal resistance of the battery is different for the law of the Arrhenius formula when the battery SOC is different. That is to say, for each SOC, the relationship between the internal resistance of the battery and the temperature is different. Therefore, for each SOC, the parameters of the Arrhenius formula of the internal resistance and temperature of the battery are different, so the above table needs to be identified by parameter identification. When the battery SOC is outside the selected 11 SOC feature points, the parameters of the required Arrhenius formula for the internal resistance and temperature of the battery can be obtained by linear interpolation. Then, in this way, the internal resistance of the battery at any SOC point and at any temperature can be obtained.

When the SOC is in [0,1] and the temperature changes within the range of [-20℃, 25℃], the relative error of the internal resistance of the battery is fitted by the Arrhenius formula as shown in the figure 9:

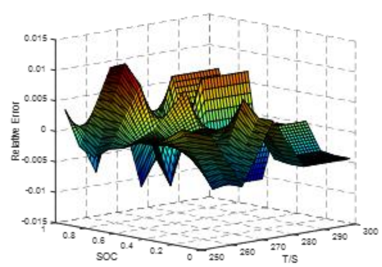

Fig 9 Relative error of internal resistance fitting at low temperature

It can be seen from the figure that the Arrhenius formula can be used to fit the internal resistance of the battery at different temperatures to obtain better accuracy, which indicates that the Arrhenius formula is suitable for the battery model below room temperature.

The parameters such as the polarization internal resistance polarization capacitance of the battery are also fitted by the Arrhenius equation. The parameters such as the polarization internal resistance polarization capacitance of the battery are also fitted by the Arrhenius equation. Therefore, these are no longer analyzed.

5. MODEL VERIFICATION

5.1 Applicability analysis of the Nernst equation and the Arrhenius formula

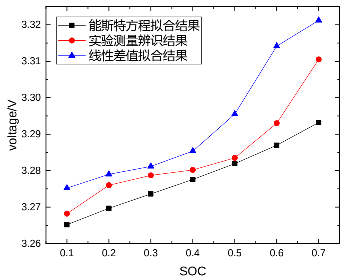

Fig 10 Comparison of fitted OCV with experimental

In this paper, the constant current discharge experiment at 15 ℃ is used to compare the Nernst equation and the Arrhenius formula with the linear interpolation method to study which method is more applicable to the model. Firstly, the applicability of the Nernst equation is analyzed. The OCV obtained by fitting the Nernst equation and the OCV obtained by linear interpolation are compared with the actually measured OCV. As can be seen from Fig. 10, it can be clearly seen that the accuracy of the Nernst equation is higher than that of the linear interpolation fit. It shows that the Nernst equation is more suitable for the model built in this paper than the linear interpolation method.

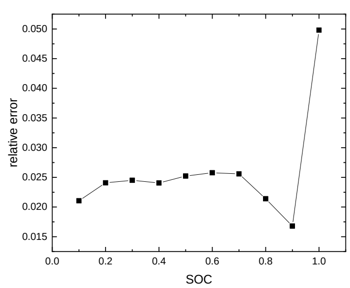

Fig 11 Linear interpolation fitting internal resistance error at -15 degree Celsius

Next, the applicability analysis of the Arrhenius equation is performed. The figure 11 shows the relative error between the internal resistance of the battery and the actual measurement with linear interpolation at -15℃. Comparing figure 11 and figure 9, the relative error of the linear interpolation fitting internal resistance is greater than 2%, while the relative error of fitting the internal resistance of the battery with the Arrhenius formula is less than 1%, so the Arrhenius equation is used. The accuracy of fitting the internal resistance of the battery is much larger than that of linear interpolation, which indicates that fitting the internal resistance of the battery with the Arrhenius formula is more suitable for the modeling of lithium iron phosphate below room temperature.

5.2 Accuracy analysis of battery low temperature model

In this paper, the constant current discharge experiment at -15℃ and the HPPC test at -15℃ were also performed. The currents of HPPC test at -10℃ and -15℃ were input as excitations into the second-order RC battery model, respectively. The error response of the model's voltage response can be obtained as follows:

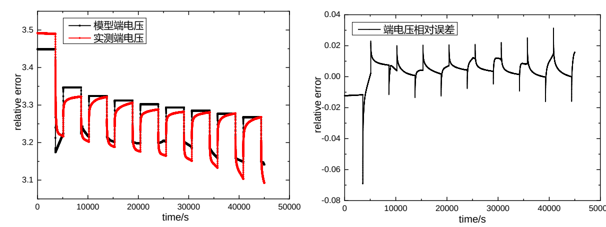

Fig 12 -10 degrees Celsius pulse discharge condition voltage and operating error curve

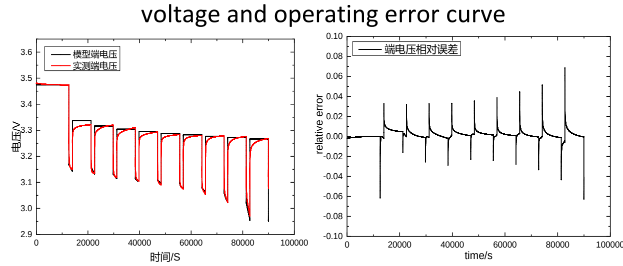

Fig 13 -15 degrees Celsius pulse discharge condition voltage and operating error curve

It can be seen from the figure that the model built in this paper has good applicability to the pulse discharge condition, but there will be a large error in the stage where the discharge just stops, the error will have a large spike, and the battery will start discharging when it is fully charged. There is a big error, because the parameters of the battery when the discharge starts from full power are more severe, and this model does not study the abrupt behavior of the model parameters when the battery starts to discharge from full power, so the error is large. For a voltage curve with a battery less than 0.9 SOC, the relative error at the peak at -10℃ is basically 2%, and the relative error at the peak at -15℃ is basically 3.5%, showing a peak at -10℃. The peak at 15℃ is small, because the feature points selected by the model contain -10℃, and the fitting of the battery parameters at this temperature is more accurate. In the battery discharge process, at -10℃ and -15℃, the relative error of the battery tracking external voltage is basically less than 1%, indicating that the battery has a good simulation ability for the discharge behavior of lithium iron phosphate battery at low temperature.

6. CONCLUSION

In this paper, the lithium iron phosphate battery is taken as the research object. The OCV-SOC curve of the battery is fitted by the Nernst equation, and the internal resistance of the battery in the Thevenin equivalent circuit model is fitted by the Arrhenius formula. Based on the SOC as a variable, the parameters such as OCV, internal resistance, polarization resistance, and polarization capacitance of the battery are taken as the SOC and temperature of the battery. The function constructs the second-order equivalent circuit model of the battery. The analysis shows that in fitting the OCV-SOC curve at different temperatures, the Nernst equation can be used to obtain better results than the linear interpolation. The accuracy of the former is significantly higher than that. the latter. The law of the internal resistance of the battery with the temperature change is also simulated by the Arrhenius formula, and compared with the linear interpolation method, the conclusion that the Arrhenius formula has better applicability is obtained. Finally, a second-order equivalent circuit model for lithium iron phosphate discharge below room temperature is established. The error is 0.1-0.9 SOC and does not exceed 5%. Within the range of 0.3-0.9 of battery SOC, the error can be less than 1%. It indicates that a model for accurately simulating the voltage variation during the discharge of lithium iron phosphate battery was successfully established.

ACKNOWLEDGEMENT

This work is supported by the National Key R&D Program of China (Grant NO.2017YFB1201004) and the National Natural Science Foundation of China (Grant No. 51907005).

REFERENCE

[1]C. Alaoui, "Solid-state thermal management for lithium-ion ev batter-ies," IEEE Transactions on Vehicular Technology, vol. 62, no. 1, pp. 98–107, Jan 2013.

[2]J. Jaguemont, L. Boulon, and Y. Dube,´ "A comprehensive review of lithium-ion batteries used in hybrid and electric vehicles at cold temperatures," Applied Energy, vol. 164, pp. 99 – 114, 2016.

[3]Y. Ji, Y. Zhang, and C. Y. Wang, "Li-ion cell operation at low temperatures," Journal of The Electrochemical Society, vol. 160, no. 4, pp. A636–A649, 2013.

[4]S. S. Zhang, K. Xu, and T. R. Jow, "The low temperature performance of li-ion batteries," Journal of Power Sources, vol. 115, no. 1, pp. 137– 140, March 2003.

[5]K. Qian, C. Zhou, Y. Yuan, and M. Allan, "Temperature effect on electric vehicle battery cycle life in vehicle-to-grid applications," in

[6]CICED 2010 Proceedings, Sept 2010, pp. 1–6.

[7]Jiuchun Jiang, Haijun Ruan, Bingxiang Sun, Weige Zhang, Wenzhong Gao, Le Yi Wang, Linjing Zhang. A reduced low-temperature electro-thermal coupled model for lithium-ion batteries[J]. Applied Energy,2016,177.

[8]V. Singh, R. Rabaa, and C. V. Reddy, "Simulating power deliverable from a li-ion battery pack at low temperatures," Transportation Elec-trification Conference (ITEC), 2015 IEEE International, pp. 1–6, Aug 2015.

[9]H. Ruan, J. Jiang, B. Sun, W. Zhang, W. Gao, L. Y. Wang, and Z. Ma, "A rapid low-temperature internal heating strategy with optimal frequency based on constant polarization voltage for lithium-ion batteries," Applied Energy, vol. 177, pp. 771 – 782, 2016.

[10]Yinjiao Xing, Wei He, Michael Pecht, Kwok Leung Tsui. State of charge estimation of lithium-ion batteries using the open-circuit voltage at various ambient temperatures[J]. Applied Energy,2014,113.